e-J. Surf. Sci. Nanotech. Vol. 10 (2012) 437-440 Conference - ISSS-6 -

Surface Potential of MIBC at Air/Water Interface: a Molecular Dynamics Study*

C. M. Phan†
Department of Chemical Engineering, Curtin University, Perth, WA 6845, Australia,

H. Nakahara, O. Shibata, and Y. Moroi
Department of Biophysical Chemistry, Nagasaki International University, Sasebo, Nagasaki 859-3298, Japan

C. V. Nguyen and D. Chaudhary
Department of Chemical Engineering, Curtin University, Perth, WA 6845, Australia
(Received 31 January 2012; Accepted 26 June 2012; Published 25 August 2012)

The interfacial behavior of alcohols is significantly different from bulk due to amphiphilic structures. Such behavior can dramatically change the interfacial properties within the nano-scale of interfacial layer and have significant applications in industrial processes such as mineral flotation. In this study, the adsorption of MIBC (methyl isobutyl carbinol), a popular frother, was investigated by molecular dynamics. Surface potential was obtained at different surface concentration and compared to experimental data. The simulations results compared well with theoretical data using a single adjustable parameter. It has been found that the disordered water molecules contribute to surface potential more than MIBC molecules. The study demonstrates the application of MD in investigating the efficiency of frother systems.
[DOI: 10.1380/ejssnt.2012.437]

Keywords: Molecular dynamics; Air/liquid interfaces; Surface potential; MIBC

I. INTRODUCTION

Alcohol behavior at adsorption layer of the air/water surface can dramatically change the interfacial properties and significantly affect industrial processes such as flotation [1] and steam condensation [2]. For instance, the adsorption of alcohols at air/water of foam film, with critical thickness < 100 nm [3], can significantly stabilize foams, which is widely applied in chemical processes. In these processes, small variation in molecular structure, from 1-hexanol or 2-hexanol to methyl isobutyl carbinol (MIBC), can lead to dramatic effect in term of foaminess [4]. For mineral flotation, MIBC has been proved superior over other hexanol isomers as flotation frother [1]. On the other hand, MIBC is very flammable and has caused serious accidents within the industry.

Theoretically, foam stabilization by surfactants is a complicated process, which is influenced by Gibbs adsorption isotherm, dynamic adsorption, diffusion from the bulk, Marangoni effect and surface potential. As the results, there is no effective model to predict foaminess despite of widespread application in industrial processes. Consequently, a combined approach using both micro and molecular investigations is required.

Recently, molecular dynamics has been applied to predict foam liquid film [5]. On the other hand, our previous study [6] has quantified the influence of MIBC adsorption on the air/water interfacial potential, which is particularly important for double-layer charge and critical affect the disjoining pressure, thin film stabilizing and foaminess [7]. Despite of negative charge on hydrophilic group, MIBC has a positive effect on surface potential. The results indicated a complicated interaction between adsorbed MIBC and surrounding water molecules. In this study, the influence of MIBC on air/water surface potential is investigated by molecular dynamics.

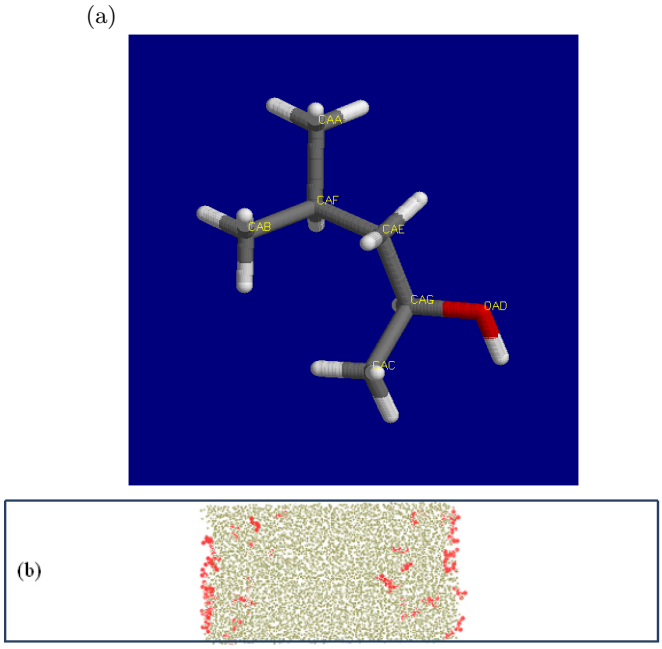

FIG. 1: Simulation: (a) molecular structure of MIBC under investigation, and (b) simulation box (gray: water, red: MIBC).

II. SIMULATION

A. Simulation parameters

A simulation box was constructed with a slab of water layer (around 9 nm thickness) placed in between two empty regions (10 nm each) as shown in Fig. 1. The

*This paper was presented at the 6th International Symposium on Surface Science –Towards Nano, Bio and Green Innovation–, Tower Hall Funabori, Tokyo, Japan, December 11-15, 2011.
†Corresponding author: c.phan@curtin.edu.au

TABLE I: Number of molecules in simulation box.

MIBCs	20	40	50	80	100
Water molecules	7271	7140	7053	6861	6714

TABLE II: Charge distribution for MIBC model.

Atom	Mass	PRGDRG charge	Modified charge
CH3	15.0350	−0.015	0
CH1	13.0190	0.031	0
CH3	15.0350	−0.016	0
CH2	14.0270	0.040	0
CH1	13.0190	0.119	0.265
CH3	15.0350	−0.004	0
O	15.9994	−0.175	−0.700
H	1.0080	0.020	0.435

simulations were performed at constant temperature T (298.15 K) and volume V in an orthorhombic simulation cell of dimensions $L_x \approx L_y \approx 5$ nm, and $L_z = 29$ nm. Molecular dynamics simulations were performed using GROMACS (version 4.4) [8] to generate the molecular trajectories using a time step of 1 fs.

The temperature was kept constant by using a Nose-Hoover thermostat with a relaxation time of 2 ps. The inhomogeneous system was first allowed to equilibrate over 500 ps, and then run for another 2 ns, which was collected for analysis. Ewald sums were used to deal with the electrostatic interactions. The most popular water potential SPC/E was used [9]. After the pure water run, the simulation procedure was repeated with different numbers of MIBC at both sides of two interfaces: 10, 20, 25, 40 and 50. The corresponding numbers of water molecules are tabulated in Table I.

B. Molecular potential

The molecular potential were obtained from PRODRG [10] using GROMOS87 forcefield. A united model of 8 atoms was used for MIBC (i.e. all hydrogen atoms, except H in hydroxyl group, are united with corresponding carbon). The charge distribution is tabulated in Table II. The original model was firstly used in simulation. However, it was found that the hydrophilic force was too small and MIBC molecules moved out of the interface.

Subsequently, the charge distribution was adjusted using the proposed distribution in the literature [11], i.e. partial charges are designated to hydroxyl group: O (−0.700), H (0.435) and alpha-C (0.265); whereas other C's are neutrally charged.

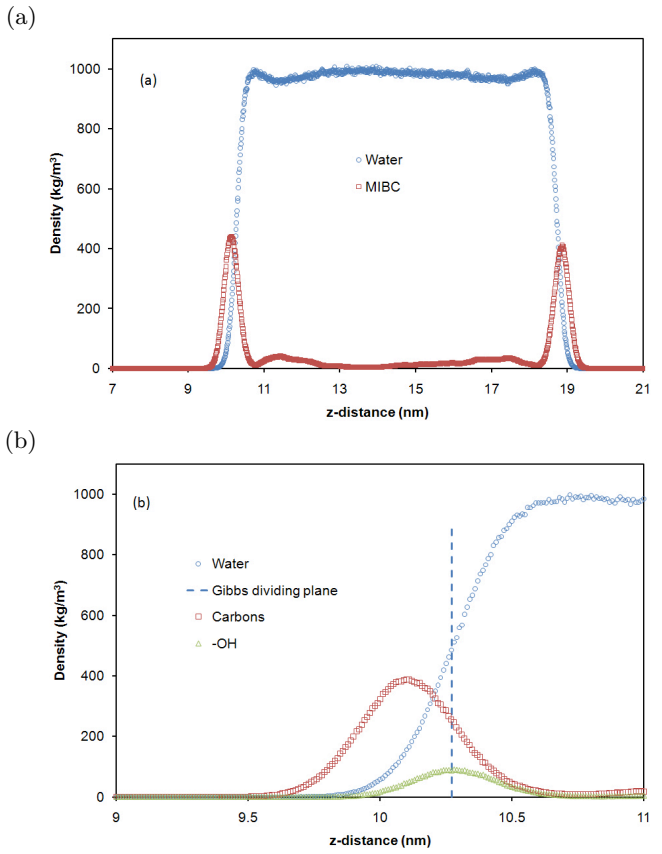

FIG. 2: Density distribution of simulation box with 40 MIBC on each side: (a) MIBC and water; and (b) distribution of hydrophobic (carbon chain) and hydrophilic (hydroxyl head) parts.

III. RESULTS AND DISCUSSION

A. Density distribution

The density distributions were calculated for water and MIBC (as shown Fig. 2(a)), hydrophobic tail (carbon chain) and hydrophilic head (–OH). Consequently, the Gibbs dividing plane was identified (i.e. plane where water interfacial excess equals to zero) as well as the position of hydrophobic and hydrophilic parts. To verify the results, the density distribution of carbon chain and hydroxyl group were analyzed relatively to the Gibbs dividing plane of water surface (Fig. 2(b)). From Figs. 2(a) and 2(b), it can be seen that MIBC is clearly distributed across the interface and thus the MIBC in simulation represented surface concentration (adsorbed concentration) not bulk concentration. The density profile also indicates no interaction between MIBC from the two opposite interfaces. Consequently, the potential of water layer represent the bulk property of the solution.

B. Surface tension

The pressure tensor was obtained from the *g_energy* provided by GROMACS. The surface tension was calcu-

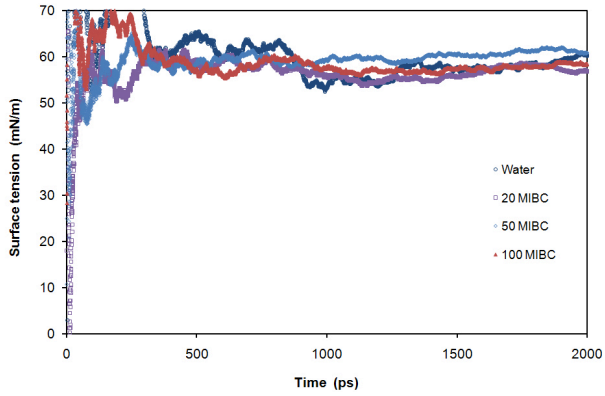

FIG. 3: Surface tension of simulated systems.

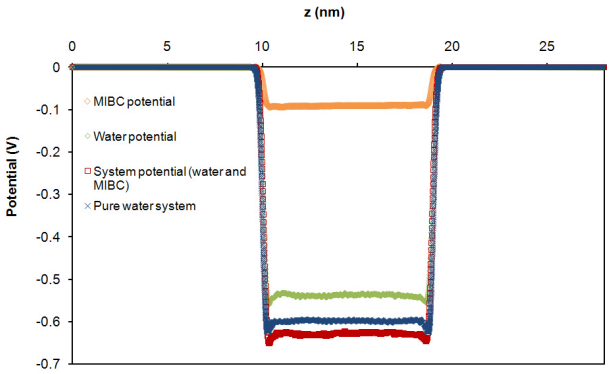

FIG. 4: Surface potential distribution along z-distance (20 MIBCs in water versus pure water).

lated using the obtained pressure tensors [12]:

$$\gamma(t) = \frac{L_z}{2}\left\{P_{zz} - \frac{P_{xx}+P_{yy}}{2}\right\}, \qquad (1)$$

where L_z is the length of the box, P_{xx}, P_{yy}, and P_{zz} are the three diagonal components of the pressure tensor along the x-, y-, and z-directions, respectively.

Subsequently, the accumulated average of surface tension was calculated as a function of time. The water surface tension was estimated at 63.7 mN/m which is similar to literature values for SPC/E: 61.3 [9] and 63.6 mN/m [12]. For alcohol simulations, however, the surface tension was very volatile and cannot be distinguished (Fig. 3). The results can be contributed to the water model or other simulation parameters. In addition to water models, the surface tension can vary with simulation size (box dimension), running time and cut-off radius. Consequently, there have been variations in reported values even for the same water model [9, 12, 13].

C. Surface potential

The surface potential was obtained for the production run using the following formula:

$$\psi(z) - \psi(0) = -\int_0^z dz' \int_0^{z'} \frac{\rho(z'')}{\varepsilon_0} dz'', \qquad (2)$$

where ε_0 is the vacuum permittivity and ρ is the charge distribution along z-axis.

Pure water has negative potential (−598 mV), which is reasonable with previous results in the literature (−546 mV) [14, 15]. As moving further inside the liquid phase, water is randomly oriented and thus the potential changes insignificantly. The negative potential indicates a unique arrangement of water molecules in the interface zone. The observation is consistent to the total dipole moment of water molecules at the interface as reported previously in the literature [13].

For MIBC/water system, the potential of MIBC and water were obtained separately. From Fig. 4, it can be seen that MIBCs generate a negative potential at the interface. This is expectable from the charge distribution between alpha-carbon and oxygen in Table I. However, MIBCs increased the potential of water, i.e. less negative in comparison to pure water system. The effect clearly demonstrates the disruption of water molecule arrangement by adsorbed MIBCs as proposed theoretically.

On the other hand, the overall surface potential, of both MIBCs and water, is more negative than that of pure water. This is contradictory to experimental data, which shown a positive influence of MIBCs on surface potential. One of the reasons for this discrepancy is oversimplification of MIBCs molecular charge distribution. For instance, the hydrocarbon chain of MIBC could have more complicated charge and some carbon-carbon bonds may also contribute to system potential. It also noteworthy that water models can significant influence surface potential as well [16].

D. Comparison with experimental data

In order to verify the modeling results, the experimental data was combined with theoretical analysis. From previous study, the relative surface potential of MIBC solution in absence of ions is given by the following linear equation [6]:

$$\Delta V = N\Gamma\frac{\mu}{\varepsilon_a\varepsilon_0}, \qquad (3)$$

where N is Avogadro number, ε_a is dielectric permittivity of adsorbed layer, Γ is the surface concentration of alcohol, μ is the total normal dipole moment per MIBC molecules.

The surface concentration can be converted back to bulk concentration using Langmuir isotherm:

$$c_b = \frac{1}{K}\frac{\Gamma}{\Gamma_m - \Gamma}, \qquad (4)$$

where c_b is bulk concentration, K and Γ_m are adsorption constant as identified previously [6]. Consequently, the surface excess can be calculated from previous experimental results and plotted in Fig. 5.

In Fig. 5, it can be seen that the surface potential of water fits experimental data qualitatively. Subsequently, an empirical parameter, k, was introduced to fit the simulated results to experiment.

$$\Delta V = k\Delta V_{\text{water}}, \qquad (5)$$

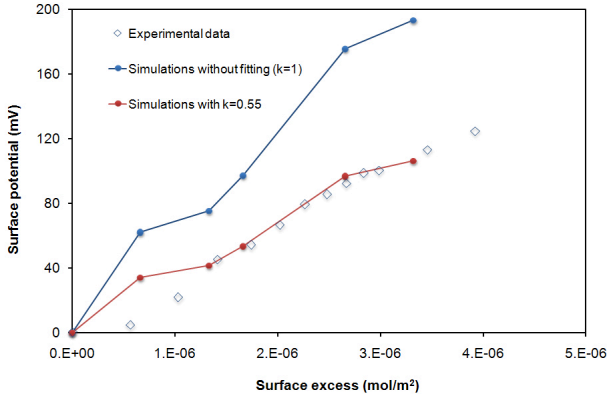

FIG. 5: Surface potential as function of MIBC surface excess: experimental data were extracted from MIBC adsorption isotherm in NaCl at 0.02 M [6].

where ΔV_{water} is the change in surface potential of water due to the presence of MIBCs.

Using linear regression, the best-fitted value of k was determined at 0.55. In Eq. (3), μ is the total normal dipole moment per MIBC molecules, which consists of two components: (i) dipole moment of adsorbed alcohols and (ii) dipole moment of water molecules disordered by alcohols [17, 18]. The fitting value ($k < 1$) implies that water disorientation, i.e. component (ii), has higher magnitude and opposite sign to dipole moment of MIBCs themselves, component (i).

If the ratio between these two components is assumed constant (i.e. the number of disordered water molecules is proportional to number of adsorbed MIBCs), then the magnitude of MIBC dipole moment is around 44% of the total dipole moment generated from disordering water molecules. It should be noted that this relationship may not hold for higher MIBC concentrations, at which a water molecule can be disordered by two or more MIBC molecules at the same time.

IV. CONCLUSIONS

The study successfully demonstrates the applicability of molecular dynamics to describe the surface potential of adsorbed MIBCs at "air"/water. The simulations highlight the significance of disordering water molecules by adsorbed MIBC molecules as hypothesized in the literature. The simulated results compared well to the experimental data using one fitting parameter. The best-fitted value, $k = 0.55$, explains the overall positive influence of MIBCs on surface potential water despite of having a negative potential themselves. The application of molecular dynamics is critical to understand the influence of molecular structure (e.g. between MIBC, 1-hexanol and 2-hexanol) on the microscopic properties of interfaces. Further investigations, both experiments and simulations, are underway to quantify the influence of alcohol structure on processes involving interfacial phenomena.

[1] R. R. Klimpel, Int. J. Miner. Process. **33**, 369 (1991).
[2] Y.-D. Jun, K. J. Kim, and J. M. Kennedy, Int. J. Refrig. **33**, 428 (2010).
[3] S. I. Karakashev, A. V. Nguyen, and E. D. Manev. J. Colloid Interface Sci. **306**, 449 (2007).
[4] B. A. Comley, P. J. Harris, D. J. Bradshaw, and M. C. Harris, Int. J. Miner. Process. **64**, 81 (2002).
[5] W. Yang and X. Yang, J. Phys. Chem. B. **115**, 4645 (2011).
[6] C. M. Phan, H. Nakahara, O. Shibata, Y. Moroi, T. N. Le, and H. M. Ang, J. Phys. Chem. B. **116**, 980 (2012).
[7] L. Wang and R.-H. Yoon. Int. J. Miner. Process. **85**, 101 (2008).
[8] B. Hess, C. Kutzner, D. van der Spoel, and E. Lindahl, J. Chem. Theory Comput. **4**, 435 (2008).
[9] F. Chen and P. E. Smith, J. Chem. Phys. **126**, 221101 (2007).
[10] A. W. Schuttelkopf and D. M. F. van Aalten, Acta Crystallographica D **60**, 1355 (2004).
[11] W. L. Jorgensen, J. Phys. Chem. **90**, 1276 (1986).
[12] C. Vega and E. de Miguel, J. Chem. Phys. **126**, 154707 (2007).
[13] P. K. Yuet and D. Blankschtein, J. Phys. Chem. B. **114**, 13786 (2010).
[14] V. P. Sokhan and D. J. Tildesley, Mol. Phys. **92**, 625 (1997).
[15] S. M. Kathmann, I. F. W. Kuo, and C. J. Mundy, J. Am. Chem. Soc. **130**, 16556 (2008).
[16] S. M. Kathmann, I. F. W. Kuo, C. J. Mundy, and G. K. Schenter, J. Phys. Chem. B. **115**, 4369 (2011).
[17] P. Warszyński, W. Barzyk, K. Lunkenheimer, and H. Fruhner, J. Phys. Chem. B **102**, 10948 (1998).
[18] H. Nakahara, O. Shibata, M. Rusdi, and Y. Moroi, J. Phys. Chem. C **112**, 6398 (2008).